Ion Acceleration Using Relativistic Pulse Shaping in Near-Critical-Density Plasmas

J. H. Bin,[1,2,*] W. J. Ma,[1,3,†] H. Y. Wang,[1–3] M. J. V. Streeter,[4] C. Kreuzer,[1] D. Kiefer,[1] M. Yeung,[5] S. Cousens,[5] P. S. Foster,[5,6] B. Dromey,[5] X. Q. Yan,[3] R. Ramis,[7] J. Meyer-ter-Vehn,[2] M. Zepf,[5,8,‡] and J. Schreiber[1,2,§]

[1]*Fakultät für Physik, Ludwig-Maximilians-Universität München, D-85748 Garching, Germany*

[2]*Max-Planck-Institute für Quantenoptik, D-85748 Garching, Germany*

[3]*State Key Laboratory of Nuclear Physics and Technology and Key Lab of High Energy Density Physics Simulation, CAPT, Peking University, Beijing 100871, People's Republic of China*

[4]*The John Adams Institute for Accelerator Science, Blackett Laboratory, Imperial College, London SW7 2AZ, United Kingdom*

[5]*Department of Physics and Astronomy, Centre for Plasma Physics, Queens University, Belfast BT7 1NN, United Kingdom*

[6]*Central Laser Facility, STFC Rutherford Appleton Laboratory, Chilton, Didcot, Oxon 0X11 0QX, United Kingdom*

[7]*E.T.S.I Aeronáuticos, Universidad Politécnica de Madrid, E-28040 Madrid, Spain*

[8]*Helmholtz-Institut-Jena, Fröbelstieg 3, 07743 Jena, Germany*

(Received 1 February 2015; published 3 August 2015)

Ultraintense laser pulses with a few-cycle rising edge are ideally suited to accelerating ions from ultrathin foils, and achieving such pulses in practice represents a formidable challenge. We show that such pulses can be obtained using sufficiently strong and well-controlled relativistic nonlinearities in spatially well-defined near-critical-density plasmas. The resulting ultraintense pulses with an extremely steep rising edge give rise to significantly enhanced carbon ion energies consistent with a transition to radiation pressure acceleration.

DOI: 10.1103/PhysRevLett.115.064801 PACS numbers: 41.75.Ak, 52.38.Kd, 52.50.Jm, 52.59.-f

Laser-driven ion accelerators provide a route to achieve high-quality ion beams (both transversely and longitudinally) with energies typically of the order of 10 s of MeV over acceleration distances of only a few micrometers. Most experiments to date have exploited target normal sheath acceleration (TNSA), in which ions from the rear surface are accelerated in strong sheath fields that are set up by energetic (hot) electrons produced by absorbing the intense laser pulse [1].

Scaling to higher beam energies and achieving quasimonoenergetic beams with reduced divergence has remained the topic of intense research. Novel acceleration modes in the relativistic transparency regime, the break-out afterburner [2], or the radiation pressure acceleration regime (RPA) [3] promise enhanced intensity scaling, preferential acceleration to high beam energy, and higher laser ion conversion efficiency, as ideally in RPA the majority of the ions in the laser focal volume are accelerated to similar velocities.

In RPA, the accelerating field is generated in an ultrathin foil target between the plasma electrons pushed by the radiation pressure of the reflected laser pulse and the ions. In contrast to TNSA, electron heating should be suppressed to avoid premature expansion of the target. This requires circularly polarized laser pulses with a sudden intensity rise. At the same time, for RPA to become the dominant acceleration mechanism requires that thinnest-possible foils remain opaque during the interaction with the very intense laser [3]—placing challenging requirements on the laser that have yet to be met by laser technology.

In principle, intensities beyond the focused intensity in vacuum coupled with a sufficiently steep rising edge can be achieved by exploiting the relativistic quiver motion of plasma electrons. The relativistic mass increase in regions of high laser intensity results in spatiotemporal nonlinearities that can lead to relativistic self-focusing [4] and pulse front steepening [5]. Laser-driven electron acceleration in underdense plasmas, for example, has benefited from the fact that initially unsuitable laser pulses are modified by relativistic nonlinearities over millimeter-length scales to the desired spatial and temporal shape to reach the bubble regime [6], resulting in GeV-electron bunches accelerated from centimeter-scale plasmas [7].

To translate this well-known concept to ion acceleration, in particular to RPA, poses the challenge of creating sufficiently uniform plasma with near-critical density (NCD) and lengths on the micrometer scale, i.e., the characteristic length scale on which the nonlinearities modify the pulse to the desired high intensity and sudden rising edge [8]. To date, it has, therefore, not been possible to exploit relativistic pulse shaping to pulses with high intensity and fast focusing geometry.

In this Letter, we demonstrate that the NCD plasmas formed using carbon nanotube foams (CNFs) [9] allow controlled shaping of laser pulses employing fast focusing optics for the first time. We apply these pulses to ion acceleration from thin diamondlike carbon (DLC) foils [10] and demonstrate significant energy increases and spectral signatures consistent with a transition to the RPA regime.

Relativistic self-focusing and pulse front steepening can be understood in terms of the spatiotemporal variation of the refractive index η due to the relativistic mass increase $m' = m_e(1 + a)$ so that $\eta = (1 - n_e/an_c)^{1/2}$ in response to a relativistically intense laser pulse with normalized vector

potential amplitude $a \gg 1$. Here, n_e and n_c are the electron and critical density of the plasma. As η is larger in the center, the plasma acts as a focusing lens and relativistic self-focusing occurs. Similar in the temporal domain, the center, high-intensity part of the pulse travels faster than the front, leading to a steepened pulse. While for weakly focused lasers, plasma densities $n_e \ll n_c$ are sufficient and easily achieved experimentally (e.g., for plasma wake-field accelerators), for ion acceleration laser pulses are typically strongly focused to focal spot diameters D_L of a few micrometers. Therefore, an at least equally strong plasma lens is required to enhance the laser further. Recently, three-dimensional particle-in-cell (PIC) simulations [8] have revealed that NCD plasmas can provide such strong focusing, well approximated by the plasma-lens f-number

$$F_{\text{no.}} = (a_0 n_c/n_e)^{1/2}. \quad (1)$$

For our experiment described below, self-focusing occurs over very short distances $f = F_{\text{no.}} D_L \approx 8\ \mu$m.

The sharp-edged, short NCD plasma is provided by employing CNF targets [9]. These can be controllably produced with thicknesses in the micrometer range, either freestanding or coated onto nanometer-thin solid foils. The CNFs in our experiment are structured on the nanometer scale (average 100 nm gap between 10 and 20 nm CNF bundles) and display uniform density on lengths scales of the laser wavelength ($\lambda_L = 0.8\ \mu$m). The average electron density for fully ionized CNF foils is estimated to be $(3.4 \pm 1.7) \times 10^{21}$ electrons/cc, i.e., $(2 \pm 1) n_c$. Here cc denotes cubic centimeter.

These novel NCD targets were investigated using the Gemini laser at the Central Laser Facility of the Rutherford Appleton Laboratory. A recollimating double plasma mirror system was introduced to enhance the laser contrast to a ratio of 10^{-9} at 5 ps before the peak of main pulse with a typical energy loss of 50%. An $f/2$ off-axis parabolic mirror was used to focus the 50 fs pulses to a full-width-at-half-maximum focal spot of $D_L \approx 3.5\ \mu$m. The energy on target after transport losses was estimated at 4–5 J, corresponding to a peak intensity of around 2×10^{20} W/cm^2 ($a_0 \approx 10$).

The performance of the CNF targets was investigated by measuring the transmitted pulses over a range of areal densities as shown in Fig. 1. Comparing the measured transmission values with results from 3D PIC simulations allows the density to be estimated in the range $(1–3) n_c$ [Fig. 1(a)]. The simulations were performed with the KLAP3D code [8] with a box size of $20 \times 20 \times 40\ \mu$m^3 sampled by $200 \times 200 \times 1600$ cells with 27 quasiparticles in each cell. The laser transmission measured through nanometer-thin solid-density DLC foils is shown for comparison. They are much smaller and consistent with the much reduced skin depth at higher plasma densities. For

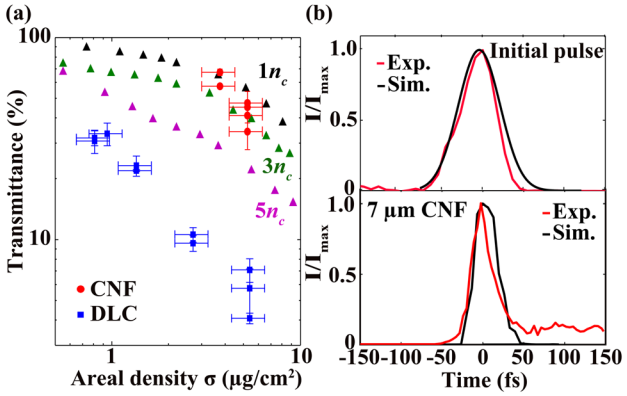

FIG. 1 (color online). (a) Laser transmittance measured through CNF (red circles) and DLC (blue squares). Main sources of errors are uncertainties in the areal density (weight) measurement and background subtraction. The triangles with different colors represent the transmission extracted from 3D PIC simulations performed for electron densities of $n_e/n_c = 1$, 3, and 5. (b) Measured and simulated temporal intensity distribution evidencing pulse front steepening through a 7 μm thick CNF target (corresponding to an areal density of $\sigma = 5.2\ \mu$g/cm^2).

both CNF and DLC, the transmission values for thicker samples are consistent with higher densities. This effect can be explained by decompression due to the prepulse affecting thinner samples more strongly.

The temporal shape of the transmitted pulses has been measured by frequency-resolved optical gating. Figure 1(b) exemplarily shows the good agreement of measured pulse shapes with simulation. In particular, the significant pulse steepening at the front ($t < 0$) is evident when comparing the incident laser pulse profile with the one transmitted through the CNF plasma. As discussed above, strong spatial self-focusing is also expected in this scenario and is clearly visible in PIC simulations (inset of Fig. 2). As a result, the laser intensity I increases as the laser is both spatially and temporally compressed in the CNF plasma and reaches peak values of $>10\times$ the peak vacuum focused intensity I_0. At the same time, the rise time reduces to $\sim$4 fs (Fig. 2). This extremely steep-rising edge accompanied with much higher peak intensity, thus, provides ideal conditions for the RPA regime.

The enhanced laser pulses were utilized for ion acceleration by coating CNF directly onto nanometer-thick DLC targets as pictured in the inset of Fig. 2. Using circularly polarized (CP) laser pulses (to suppress the competing TNSA mechanism), ion spectra were recorded with a Thomson parabola spectrometer for different CNF thicknesses. The energies increase with increasing CNF thickness, and best performance is observed for the largest CNF thickness. The corresponding energy distributions of protons and C^{6+} ions in Fig. 3(a) reveal that carbon acceleration benefits most with an increase in maximum energy of 2.7 times over an uncoated DLC foil. By contrast, proton

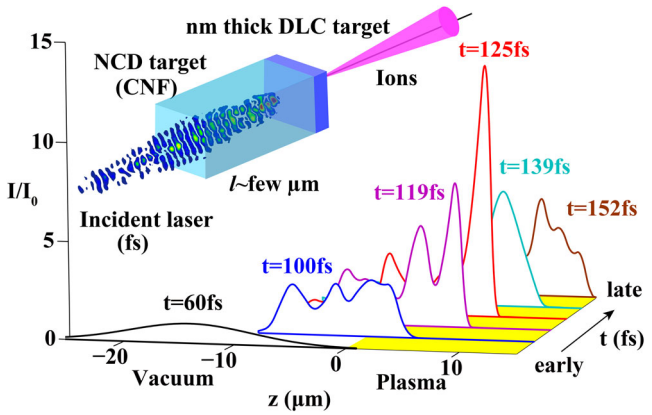

FIG. 2 (color online). On-axis intensity-envelope distribution extracted from 3D PIC simulations at different times. The circularly polarized ASTRA Gemini-laser pulse propagates through a NCD plasma with electron density $n_e = 2n_c$ (yellow area). The pulse rise time shortens to ~4 fs. The peak intensity multiplies by a factor of 10, mainly due to relativistic self-focusing as shown in the 2D intensity map at $t = 125$ fs (inset). Placing a micron-scale layer of NCD in front of a DLC foil (inset) allows the enhanced pulse to be exploited for laser ion acceleration.

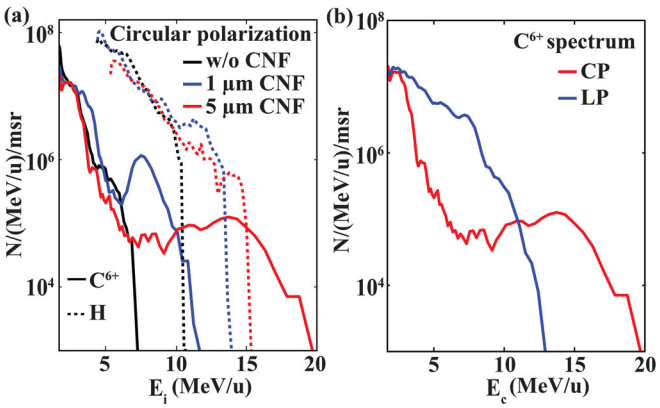

FIG. 3 (color). (a) Energy distributions of C^{6+} ions (solid curves) and protons (dashed curves) registered from DLC foils combined with CNF targets of varying thicknesses irradiated by circularly polarized laser pulses. (b) C^{6+} ion spectrum under best conditions for CP (red) and LP (blue).

energies increased by a factor of only 1.5. Moreover, the shape of the carbon spectra deviates from monotonically decaying, especially at around 70% of the maximum energy. Similar observations have previously been associated with RPA [11,12]. Further support for this interpretation is that the energy per nucleon of carbon ions increases more rapidly than the proton energy and eventually becomes comparable; i.e., the fastest ions travel with similar velocities [3]. It is also noteworthy that the observed maximum carbon energy ~20 MeV/u is, to the best of our knowledge, the highest value for carbon ions demonstrated from a Gemini-class laser system to date.

For the above discussion, it is important to note that although carbon ions were observed when irradiating freestanding CNF targets, their energy and number were insignificant. In the detectable spectral range of 2–50 MeV/u, no proton trace was observed, and only carbon ions with lower maximum energy of about 3.5 MeV/u with $\sim 10^3$ lower yield were observed, suggesting that the role of the CNF is, indeed, mainly to provide a medium for modifying the laser pulse to the desired shape. By contrast, linearly polarized (LP) laser pulses result in invariably monotonically decaying spectra, both for protons and carbon ions. One example is shown in Fig. 3(b), where the difference in the spectrum of C^{6+} ions with different polarizations is clearly visible. Again, the energies increased with increasing CNF thickness. Here, proton energies were enhanced more strongly from 12 to 29 MeV by a factor of 2.4, while C^{6+} energies by a smaller factor of 1.7.

To validate our hypothesis further, we performed detailed 3D PIC simulations. Because of the multiscale nature of the problem, i.e., micrometer-long plasma with low density and a nanometer-thin, high-density foil, we needed to simplify the problem by dividing the simulation into two steps. First, the propagation of the Gemini-laser pulse through a NCD plasma with electron density of $2n_c$ (resembling the CNF plasma) was simulated, and the complete resulting electromagnetic field was extracted at different depths within the NCD plasma. This field was then fed into a second simulation with a single DLC foil. A high-density plasma slab (60 nm, $100n_c$, C:H = 9:1 in number density, initial temperature of 1 keV) was used to represent a DLC foil with the reduced density allowing for any initial decompression during the early stages of the interaction and also reducing the computational requirements. In the second series, the simulation box was subdivided into a grid of $200 \times 200 \times 4000$ cells to resolve the DLC thickness.

The limitation of this approach is that fast electrons produced within the NCD plasma do not contribute to the ion acceleration at the DLC foil. Consequently, we may underestimate the sheath fields at the rear, which would preferentially accelerate the protons via the TNSA mechanism. However, the good agreement of our current simulations with the data described below suggests that the approximation inherent in our numerical approach only has a minor impact.

In agreement with the experimental results, we observe a significant increase of the maximum C^{6+} ion energy with increasing CNF thickness. The ratio of these energies to the energy obtained for a plain DLC foil defines the enhancement factor α and is plotted against CNF thickness in Fig. 4(a). The general trend of both the experiment and simulation results agrees very well and suggests that we have not even explored the full capacity of the scheme in the parameter range accessed in our experiment. Our simulations predict a fourfold increase in energy obtainable

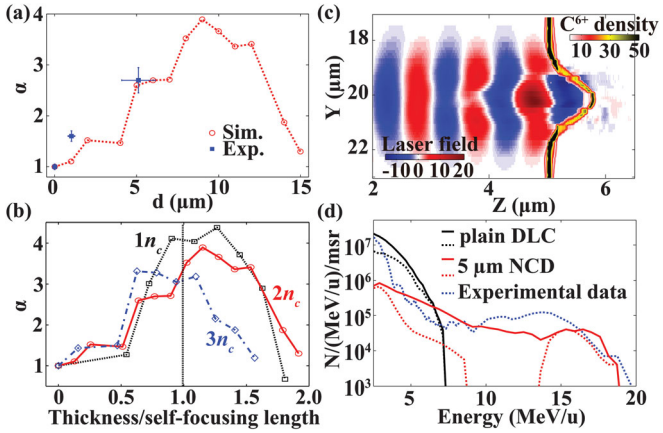

FIG. 4 (color). 3D PIC simulation results. (a) The carbon energy increases with NCD length. (b) Simulations with three different electron densities evidence that self-focusing length optimizes ion acceleration. (c) 2D density map of C^{6+} ions and laser field distribution at $t = 100$ fs for the 5 μm NCD case, best performance in experiments. (d) C^{6+} ion energy spectra from simulation of 5 μm NCD + DLC (red) and from the plain DLC foil (black) considering all the ions (solid) and ions originating from the back facing 1/3 of the foil in the focal volume (dashed). The measured spectrum (blue dashed) is shown for comparison.

using a $2n_c$ plasma with 9 μm length under our conditions. At this point, the laser is predicted to have reached its highest intensity via self-focusing. The self-focusing length in the simulation agrees well with the simple estimate of Eq. (1), $f = F_{\text{no.}} D_L \approx 8$ μm. When performing the same set of simulations with NCD plasma densities of $1n_c$ and $3n_c$ and otherwise identical parameters, ion acceleration is optimized when the NCD thickness corresponds to the respective self-focusing length [Fig. 4(b)]. This suggests that the effect of the NCD plasma is robust to variation of the exact density and that the observed carbon energy increase is primarily due to the enhanced laser pulse interacting with the DLC foil.

The strong enhancement of carbon ion energies for circular polarization (as compared to linear polarization), the significantly altered spectral shape, and the fact that protons and carbon ions reach similar velocities provide strong evidence that the RPA contribution to the acceleration process is becoming stronger with increasing CNF thickness. The carbon spectra in Fig. 3(b) also show a significant peak, which is not observed for linear polarization.

Numerical investigations [3] suggest that RPA is more likely to dominate over TNSA in the limit of high intensities for circularly polarized laser pulses at normal incidence, as these should suppress the electron heating required for TNSA. In tight focusing experiments with thin foils, however, this advantage is generally not observed due to strong radial intensity gradients which results in rapid foil deformation and a comparable hot electron production regardless of polarization state [13]. For a given laser intensity and spot size, this deformation can be reduced by using pulses with a steeper rising edge. In our situation, the steepened pulse front significantly reduces the time available for deformation to take place. This results in slower decompression of the foil and an increased RPA contribution.

Indeed, the above interpretation is confirmed by the 3D PIC simulation results. Figure 4(c) shows the 2D (Y-Z) density map of C^{6+} ions extracted from simulations. The carbon ions are accelerated in a manner typical of RPA with the modified pulse: the foil is accelerated as a whole and remains highly overdense while its shape closely resembles the transverse laser profile. The target remains highly reflective with almost no transmitted laser energy, which is well in line with the measured overall few-percentage laser transmission. The resulting nonexponential distribution [Fig. 4(d), red solid line] agrees not only qualitatively but also quantitatively with the measured spectrum (blue dashed). In particular, the high-energy spectral peak can be seen to be formed by the ions in the focal volume in a thin layer in the rear side of the target (red dashed). This is consistent with a previous theoretical investigation [14], which shows that only a thin layer at the target rear in the focal volume forms the monoenergetic feature during RPA. By contrast, the C^{6+} ions spectra for a plain DLC foil with the unmodified pulse results in quasiexponential spectra consistent with TNSA dominating.

In conclusion, we have demonstrated the practical feasibility of ultrathin CNF foams to realize relativistic self-focusing and pulse front steepening at the same time. This has allowed us to accelerate ions from nanometer-thin DLC targets to substantially higher energies, about a factor of 3, which would otherwise require much larger lasers. We have observed preferential enhancement of the carbon ion energies for circular polarization, consistent with a stronger RPA contribution to the overall acceleration. The demonstration of controlled, micrometer-length NCD plasmas will have significant impact on related experiments with high-intensity laser pulses, covering acceleration of dense electron bunches [15], generation of large (electro)magnetic fields [16,17], and the production of intense, high-energy radiation [18].

The work was supported by the DFG Cluster of Excellence Munich-Centre for Advanced Photonics (MAP) and the Transregio TR18, as well as the International Max Planck Research School of Advanced Photon Science (IMPRS-APS). The experiment was funded by EPSRC and the A-SAIL and LIBRA grants. X. Q. Y. and H. Y. W. are supported by National Basic Research Program of China (Grant No. 2013CBA01502). We thank the staff of the ASTRA Gemini operations team and the CLF for their assistance during the experiment.

*jianhui.bin@physik.uni-muenchen.de
†wenjun.ma@physik.uni-muenchen.de

[‡]m.zepf@qub.ac.uk
[§]Joerg.Schreiber@lmu.de

[1] S. C. Wilks, A. B. Langdon, T. E. Cowan, M. Roth, M. Singh, S. Hatchett, M. H. Key, D. Pennington, A. MacKinnon, and R. A. Snavely, Phys. Plasmas **8**, 542 (2001).

[2] L. Yin, B. J. Albright, B. M. Hegelich, and J. C. Fernández, Laser Part. Beams **24**, 291 (2006); L. Yin, B. J. Albright, B. M. Hegelich, K. J. Bowers, K. A. Flippo, T. J. T. Kwan, and J. C. Fernández, Phys. Plasmas **14**, 056706 (2007); L. Yin, B. J. Albright, K. J. Bowers, D. Jung, J. C. Fernández, and B. M. Hegelich, Phys. Rev. Lett. **107**, 045003 (2011).

[3] A. Macchi, F. Cattani, T. V. Liseykina, and F. Cornolti, Phys. Rev. Lett. **94**, 165003 (2005); X. Q. Yan, C. Lin, Z. M. Sheng, Z. Y. Guo, B. C. Liu, Y. R. Lu, J. X. Fang, and J. E. Chen, Phys. Rev. Lett. **100**, 135003 (2008); O. Klimo, J. Psikal, J. Limpouch, and V. T. Tikhonchuk, Phys. Rev. ST Accel. Beams **11**, 031301 (2008); A. P. L. Robinson, P. Gibbon, M. Zepf, S. Kar, R. G. Evans, and C. Bellei, Plasma Phys. Controlled Fusion **51**, 024004 (2009); B. Qiao, M. Zepf, M. Borghesi, and M. Geissler, Phys. Rev. Lett. **102**, 145002 (2009).

[4] M. Borghesi, A. J. MacKinnon, L. Barringer, R. Gaillard, L. A. Gizzi, C. Meyer, O. Willi, A. Pukhov, and J. Meyer-ter-Vehn, Phys. Rev. Lett. **78**, 879 (1997).

[5] C. E. Max, J. Arons, and A. Bruce Langdon, Phys. Rev. Lett. **33**, 209 (1974); J. Schreiber, C. Bellei, S. P. D. Mangles, C. Kamperidis, S. Kneip, S. R. Nagel, C. A. J. Palmer, P. P. Rajeev, M. J. V. Streeter, and Z. Najmudin, Phys. Rev. Lett. **105**, 235003 (2010).

[6] C. G. R. Geddes, Cs. Toth, J. van Tilborg, E. Esarey, C. B. Schroeder, D. Bruhwiler, C. Nieter, J. Cary, and W. P. Leemans, Nature (London) **431**, 538 (2004); J. Faure, Y. Glinec, A. Pukhov, S. Kiselev, S. Gordienko, E. Lefebvre, J.-P. Rousseau, F. Burgy, and V. Malka, Nature (London) **431**, 541 (2004); S. P. D. Mangles, C. D. Murphy, Z. Najmudin, A. G. R. Thomas, J. L. Collier, A. E. Dangor, E. J. Divall, P. S. Foster, J. G. Gallacher, C. J. Hooker, D. A. Jaroszynski, A. J. Langley, W. B. Mori, P. A. Norreys, F. S. Tsung, R. Viskup, B. R. Walton, and K. Krushelnick, Nature (London) **431**, 535 (2004).

[7] W. P. Leemans, B. Nagler, A. J. Gonsalves, Cs. Tóth, K. Nakamura, C. G. R. Geddes, E. Esarey, C. B. Schroeder, and S. M. Hooker, Nat. Phys. **2**, 696 (2006); X. Wang *et al.*, Nat. Commun. **4**, 1988 (2013).

[8] H. Y. Wang, C. Lin, Z. M. Sheng, B. Liu, S. Zhao, Z. Y. Guo, Y. R. Lu, X. T. He, J. E. Chen, and X. Q. Yan, Phys. Rev. Lett. **107**, 265002 (2011).

[9] W. Ma, L. Song, R. Yang, T. Zhang, Y. Zhao, L. Sun, Y. Ren, D. Liu, L. Liu, J. Shen, Z. Zhang, Y. Xiang, W. Zhou, and S. Xie, Nano Lett. **7**, 2307 (2007).

[10] W. Ma, V. Kh. Liechtenstein, J. Szerypo, D. Jung, P. Hilz, B. M. Hegelich, H. J. Maier, J. Schreiber, and D. Habs, Nucl. Instrum. Methods Phys. Res., Sect. A **655**, 53 (2011).

[11] A. Henig *et al.*, Phys. Rev. Lett. **103**, 245003 (2009).

[12] S. Kar *et al.*, Phys. Rev. Lett. **109**, 185006 (2012).

[13] F. Dollar *et al.*, Phys. Rev. Lett. **108**, 175005 (2012).

[14] A. Macchi, S. Veghini, and F. Pegoraro, Phys. Rev. Lett. **103**, 085003 (2009).

[15] D. Kiefer *et al.*, Nat. Commun. **4**, 1763 (2013).

[16] A. Pukhov and J. Meyer-ter-Vehn, Phys. Rev. Lett. **76**, 3975 (1996).

[17] R. J. Mason and M. Tabak, Phys. Rev. Lett. **80**, 524 (1998).

[18] B. Dromey, S. Rykovanov, M. Yeung, R. Hörlein, D. Jung, D. C. Gautier, T. Dzelzainis, D. Kiefer, S. Palaniyppan, R. Shah, J. Schreiber, H. Ruhl, J. C. Fernandez, C. L. S. Lewis, M. Zepf, and B. M. Hegelich, Nat. Phys. **8**, 804 (2012).